Cell, Vol. 106, 429–441, August 24, 2001, Copyright ©2001 by Cell Press

Crystal Structure of the Processivity Clamp Loader Gamma (γ) Complex of *E. coli* DNA Polymerase III

David Jeruzalmi, Mike O'Donnell, and John Kuriyan[1]
Howard Hughes Medical Institute
The Rockefeller University
1230 York Avenue
New York, New York 10021

Summary

The γ complex, an AAA+ ATPase, is the bacterial homolog of eukaryotic replication factor C (RFC) that loads the sliding clamp (β, homologous to PCNA) onto DNA. The 2.7/3.0 Å crystal structure of γ complex reveals a pentameric arrangement of subunits, with stoichiometry δ′:γ_3:δ. The C-terminal domains of the subunits form a circular collar that supports an asymmetric arrangement of the N-terminal ATP binding domains of the γ motor and the structurally related domains of the δ′ stator and the δ wrench. The structure suggests a mechanism by which the γ complex switches between a closed state, in which the β-interacting element of δ is hidden by δ′, and an open form similar to the crystal structure, in which δ is free to bind to β.

Introduction

The β subunit of the DNA Polymerase III holoenzyme confers upon the polymerase the ability to faithfully track the rapidly moving replication fork while synthesizing leading and lagging strand DNA simultaneously (reviewed in Kelman and O'Donnell, 1995). The β subunit, known as a sliding clamp, forms a stable ring-shaped structure that encircles DNA (Kong et al., 1992; Stukenberg et al., 1991). Once attached to the β subunit, the catalytic α subunit of the polymerase can move along DNA for tens of kilobases or more without dissociation, incorporating new nucleotides into the growing DNA strand at speeds as high as 750 nt/s (Naktinis et al., 1996; Stukenberg et al., 1991). The sliding clamps and their associated clamp loading systems are of broad importance in many cellular processes involving DNA, beyond that originally envisaged by their discovery as essential factors for chromosomal replication.

The partitioning of the polymerase complex into separate components that deal with chemical catalysis and processivity is a feature common to the chromosomal replicases of eubacteria, archaebacteria, eukaryotes, and T4 bacteriophage (Stillman, 1994; Young et al., 1992). Such a mechanism allows these polymerases to cope with the opposite directionality of the two DNA strands emerging from the moving replication fork. In *E. coli*, the DNA polymerase III holoenzyme contains two complexes of the catalytic α-ε polymerase/exonuclease subunits (McHenry, 1982; Studwell-Vaughan and O'Donnell, 1991), as originally proposed in the "trombone model" for the replication fork (Alberts et al., 1983) (Figure 1A). For the holoenzyme assembly to rapidly track the advancing replication fork, both α-ε complexes need to move forward in a coupled manner. As the leading strand polymerase tracks a spiral path along DNA, it must pull the lagging strand polymerase with it, rotating it by 360° about eight times each second. To avoid the tangle that would otherwise result, the polymerase can release DNA, holding onto the fork via attachment to β. This would allow the leading strand DNA to swivel back into position within the β clamp (Hingorani and O'Donnell, 2000).

While the leading strand polymerase can remain bound to a β dimer continuously, the lagging strand polymerase repeatedly initiates DNA synthesis on new Okazaki fragments, each of which is extended for ~1000 bases. Sliding clamps allow the lagging strand polymerase/exonuclease to hop from a completed Okazaki fragment to one that has been newly primed (O'Donnell, 1987; Stukenberg et al., 1994).

The β clamp is loaded onto DNA by clamp loader complexes consisting of a minimum of three kinds of subunits (γ, δ′, and δ) (Onrust et al., 1995a), with recent data favoring a stoichiometry of γ_3:δ′:δ (Pritchard et al., 2000). We refer to this assembly as the γ complex. In *E. coli*, a protein known as τ, which is identical to γ except for the addition of a C-terminal segment, is produced from the same *DnaX* gene as is γ (Flower and McHenry, 1990; Tsuchihashi and Kornberg, 1990). The additional segment in τ is required for the inclusion of two copies of the catalytic core assembly within the DNA polymerase III holoenzyme (Onrust et al., 1995b; Studwell-Vaughan and O'Donnell, 1991) and for interaction with the DnaB helicase (Kim et al., 1996; Yuzhakov et al., 1996), but is not required for clamp loading.

The γ subunits of the complex are the motor proteins that bind ATP and undergo substantial (but undefined) conformational changes as a consequence of nucleotide binding and hydrolysis (Hingorani and O'Donnell, 1998; Naktinis et al., 1995). Ring opening requires the δ subunit wrench, which has affinity for the β subunit on its own (Naktinis et al., 1995) (see accompanying paper, Jeruzalmi et al., 2001 [this issue of *Cell*]). The δ′ subunit appears to be a conformationally stable stator and is the only subunit whose structure has been determined in isolation (Guenther et al., 1997). The γ, δ, and δ′ subunits are all structurally related to the AAA+ ATPases (Jeruzalmi et al., 2001; Neuwald et al., 1999).

The eukaryotic sliding clamp protein, PCNA, is structurally similar to the eubacterial β subunit (Gulbis et al., 1996; Krishna et al., 1994). The clamp loading function in eukaryotes is carried out by a clamp loader complex known as replication factor C (RFC) (Stillman, 1994). There are five RFC subunits in eukaryotes (RFC 1–5), all of which share sequence similarity to the eubacterial γ and δ′ subunits (Cullman et al., 1995; Guenther et al., 1997; O'Donnell et al., 1993). ATP-dependent conformational changes in RFC have been visualized at low resolution by electron microscopy and atomic force microscopy (Shiomi et al., 2000). Additionally, Morikawa and

[1] Correspondence: kuriyan@rockefeller.edu

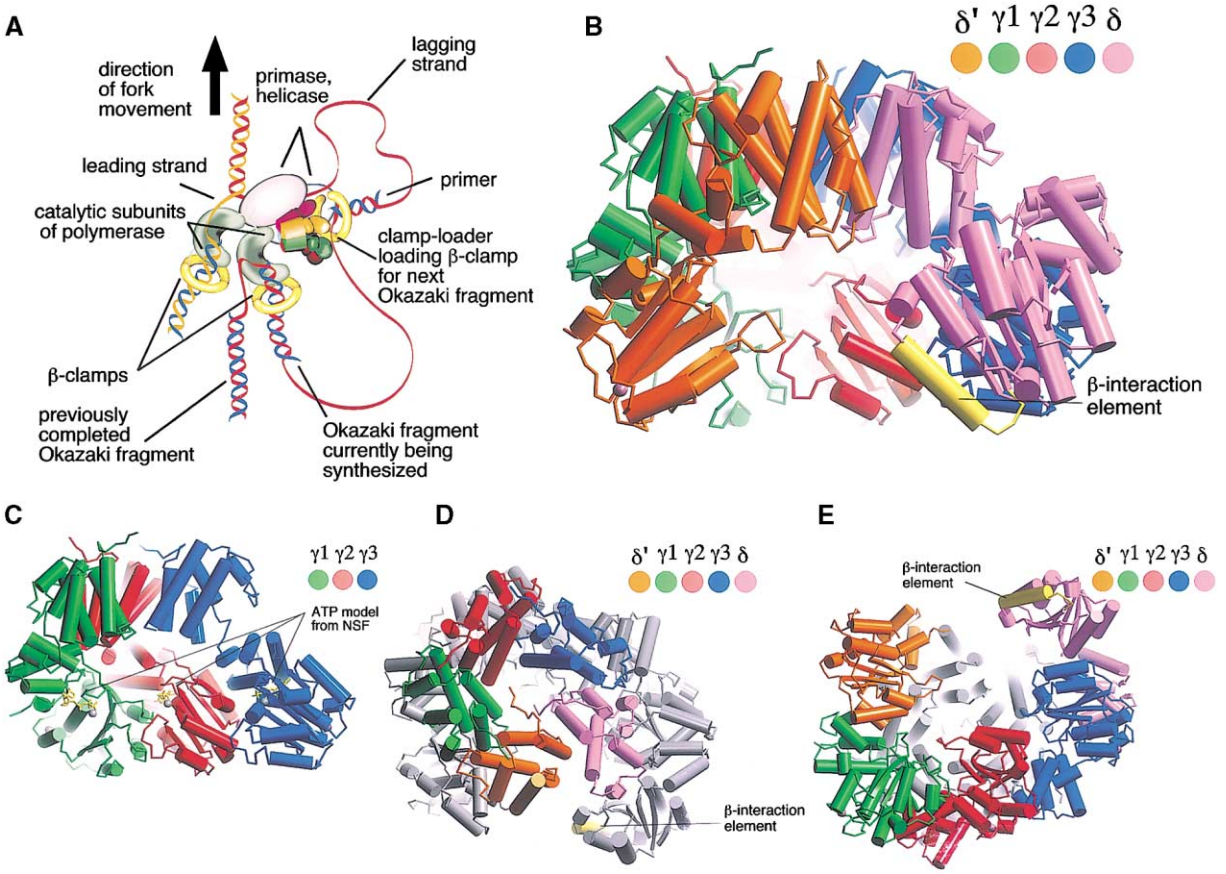

Figure 1. Structure of the γ Complex

(A) Schematic representation of DNA polymerase III holoenzyme at a replication fork.

(B) Front view of the γ complex.

(C) The same view as in (B), but with δ and δ′ removed. The ATP analog AMP-PNP is shown, based on the structure of NSF-D2 (Lenzen et al., 1998; Yu et al., 1998).

(D) Top view of the γ complex, emphasizing the structure of the C-terminal helical collar. The other domains of each subunit are colored gray for clarity.

(E) Bottom view, showing the asymmetrical disposition of the N-terminal domains. The β-interacting element of δ is colored yellow.

coworkers have recently determined the structure of the small subunit from the RFC of the archaebacterium *Pyrococcus furiosus*. The subunit architecture and the intersubunit packing seen in the archael structure is similar to that seen in the bacterial clamp loader described below (Oyama et al., 2001 [August issue of *Molecular Cell*]). The clamp loader of the T4 bacteriophage DNA polymerase system has been extremely well studied (Young et al., 1992). The sliding clamp of T4 bacteriophage, the gp45 protein, is structurally similar to both β subunit and PCNA (Moarefi et al., 2000; Shamoo and Steitz, 1999). The clamp loader consists of the gp62 and gp44 proteins, and sequence similarity between gp62, γ, and RFC subunits suggests a common mechanism of action.

In order to understand the mechanism of clamp loading at the molecular level, we have determined the crystal structure of γ complex, containing the γ, δ′, and δ subunits, at 2.7/3.0 Å resolution. The clamp loader complex is assembled from five subunits, each with the same fold. Nevertheless, each subunit in the complex adopts a very different conformation due to differences in their interdomain arrangements. The striking asymmetry in the structure allows us to extrapolate from this crystal structure of a nucleotide-free form of the γ complex to the structural transitions that result in the loading of the β ring on DNA.

Results and Discussion

We first describe the features of the γ complex that are derived directly from the crystal structure. Then, commencing with the section entitled "Implications for Structural Transitions in the γ Complex," we discuss models for a closed, more symmetric, and nucleotide-free conformation of the γ complex. We have also built a model that is slightly more open than that seen in the crystal structure and to which the β subunit can be docked. These concluding sections are speculative, but are motivated by biochemical insights into the clamp loading process in *E. coli* (see, for example, Turner et al., 1999).

Structure Determination

A form of the γ complex that is fully active in clamp loading was prepared by reconstituting purified δ, δ′,

and a truncated γ subunit (residues 1–373; see Experimental Procedures). The crystal structure of the γ complex was determined using X-ray data extending anisotropically to 2.7/3.0 Å spacings. The crystallographic asymmetric unit contains one γ complex, of molecular mass 200 kDa, consisting of 3 γ subunits and one each of the δ and δ′ subunits. A complete model has been built and refined for all parts of the structure, with the exception of two short segments in the C-terminal domain of δ, to free and working R values of 30.4% and 26.1%, respectively (Table 1).

General Description of the Structure

The γ complex is assembled as a heteromeric pentamer with stoichiometry δ′:γ_3:δ (Figure 1B). Each of the subunits has the same overall fold as δ′, including an N-terminal RecA-like fold (Domain I), followed by two helical domains (Domains II and III). The C-terminal helical domains form a ring-shaped collar in the upper part of the assembly, in which the δ′ and δ subunits pack against each other and bracket three γ subunits (Figure 1D). The relative orientations of the three component domains are different in each of the five subunits, resulting in a highly asymmetric structure, particularly in the lower part of the assembly (Figure 1E). The five N-terminal domains do not form a closed circular structure, and are instead arranged in an open σ shape, with the N-terminal domain of the δ subunit being displaced outward the most. The γ subunits are so arranged that the nucleotide binding sites face the inner surface of the γ complex, and are not visible from the outside (Figure 1C).

Crystal packing interactions are likely to be responsible for the highly asymmetrical structure seen in the crystal, in which the β interaction elements of δ are completely exposed at the outer extremity of the assembly. The distal tip of Domain I of δ interacts extensively with another molecule in the crystal, as does Domain I of δ′. The crystal thus appears to hold the γ complex open.

The Structure of the ATP Binding Domain of the γ Subunit

Domain I of the γ subunit has a "P loop" type nucleotide binding fold (Walker et al., 1982), which has central elements in common with many ATPases and GTPases, including F_1-ATPase, RecA, Ras, and heterotrimeric G proteins (Guenther et al., 1997). Domains I and II together form a structural unit that is common between γ, δ, and δ′ and members of the large family of proteins known as AAA+ ATPases (Neuwald et al., 1999). The C-terminal helical Domain III is unique to the clamp loaders amongst the AAA+ proteins of known structure.

The AAA+ family of ATPases is an extension of the AAA (for *A*TPases *a*ssociated with a variety of cellular *a*ctivities) family, originally defined to include proteins with a common ~200 residue ATPase core that are involved in a variety of functions, such as protein degradation (chaperones associated with proteosomes) or vesicular fusion (the N-ethylmaleimide-sensitive fusion protein, NSF) (May et al., 2001; Neuwald et al., 1999). The extended AAA+ family includes the clamp loader subunits, such as γ, as well as replication proteins such as the MCMs and cdc6 (Liu et al., 2000; May et al., 2001; Neuwald et al., 1999). The first structures for members of the AAA+ family were determined for δ′ (Guenther et al., 1997) and for the D2 domain of NSF (Lenzen et al., 1998; Yu et al., 1998). Subsequently, the structures of several other AAA+ ATPases have been determined (for a recent review, see May et al., 2001).

While the γ subunit structure has been determined in the absence of nucleotides, the binding mode of ATP can be determined reliably because of the structural correspondence between Domains I and II of γ and the structures of the AAA+ ATPases bound to nucleotides. The NSF protein contains two ATP binding domains, D1 and D2, that are arranged in concentric hexameric rings (while D1 is an ATPase, the D2 domain is not). We use the structure of the D2 domain of NSF (NSF-D2), which has been determined in the presence of ATP (Yu et al., 1998) and the ATP analog AMP-PNP (Lenzen et al., 1998), and also that of the NSF homolog p97, complexed with ADP (Zhang et al., 2000), for comparison to γ. While the level of sequence similarity between the N-terminal domain of γ and NSF is not particularly high, the region around the nucleotide is structurally similar in both proteins. Of 87 residues in a structurally matched core between NSF-D2 and γ, only 18 are identical, but the rms deviation for this matched core is 1.8 Å.

The three nucleotide binding domains of γ are indistinguishable at the resolution of the present analysis. The domains are free of nucleotide, although a sulfate ion is bound near the P loop in each case. The nucleotide binding domains of AAA+ ATPases have been discussed extensively (May et al., 2001), and the only unusual feature of the γ subunit is the presence of a zinc binding module that is inserted between α2 and α3 (see Figure 1 of Jeruzalmi et al., 2001). The RFC and δ subunits lack this zinc module, and its function is unknown.

The Sensor 1 and Sensor 2 elements of AAA+ ATPases are implicated in the transmission of conformational changes in response to ATP binding (Guenther et al., 1997; May et al., 2001; Neuwald et al., 1999). In γ, the Sensor 1 region includes the loop following strand β4 and helix α7 (residues 157–170), and corresponds to the region known as Switch 2 in G proteins (Vetter and Wittinghofer, 1999). Ser-655 in NSF-D2 (numbering as in Lenzen et al., 1998), corresponding to Thr-157 in γ, forms a hydrogen bond with the terminal phosphate of AMP-PNP. There are as yet no structures of the same AAA+ ATPase protein bound to both ADP and ATP, and so a reliable view of the response of Sensor 1 to ATP binding in any of these proteins is not available. However, comparison with the structures of G proteins and ATP binding motor proteins suggests that movement of the Sensor 1 loop (Switch 2 in G proteins) toward the terminal phosphate of ATP upon ATP binding will result in a correlated movement of helix α7 (Vetter and Wittinghofer, 1999). In γ, helix α7 in the Sensor 1 region bears at its C terminus three residues (Ser-168, Arg-169, and Cys-170) that form an "SRC" motif that is conserved in clamp loader subunits throughout all branches of life (Cullman et al., 1995; O'Donnell et al., 1993).

The Sensor 2 motif is located in the N-terminal region of helix α9 in Domain II. Lys-716 in the Sensor 2 motif of NSF-D2 interacts with the phosphates of ATP or AMP-PNP. In the γ subunit structures, the orientation of Domain II with respect to Domain I positions the corresponding Arg-215 somewhat differently. In γ3, for

Table 1. Crystallographic Statistics

$\gamma_3\delta\delta'$ complex (Space group: $P2_12_12_1$, Cell parameters: a = 95.70 Å, b = 95.86 Å, c = 285.41 Å, $\alpha = 90$, $\beta = 90$, $\gamma = 90$)
Experimental Phasing Analysis:

Dataset	Resolution Å	Reflections (Measured/Unique)	Completeness	R_{sym}[a]	Phasing Power[b] iso/ano
TaBr-MAD (Ta inflection pt: $\lambda = 1.25520$) (ALS)	20–3.35	487,811 73,154	99.2	6.7	0.44
TaBr-MAD (Ta peak: $\lambda = 1.25490$) (ALS)	20–3.35	229,008 38,452	99.0	8.3	0.76
Figure of merit[c]: 0.16	20–3.5				
TaBr-MAD (Ta inflection pt: $\lambda = 1.2550$) (SSRL)	20–4.3	412,397 18,086	99.3	12.8	
TaBr-MAD (Ta peak pt: $\lambda = 1.25400$) (SSRL)	20–4.3	534,326 22,460	99.5	21.2	0.85
TaBr-MAD (high energy: $\lambda = 1.21800$) (SSRL)	20–4.3	424,682 18,079	99.3	12.1	1.14
Figure of merit[c]: 0.50	20–4.5				
Native ($\lambda = 1.03320$) (SBC-APS)	20–3.7	398,344 27,405	96.5	7.9	
U-MAD (U peak: $\lambda = 1.7215$) (SBC-APS)	20–4.5	198,182 16,212	98.5	8.4	0.45
U-MAD (low energy: $\lambda = 0.9902$) (SBC-APS)	20–4.5	201,139 16,257	98.8	12.0	0.48/0.91
Figure of merit[c]: 0.10/0.04	20–4.5				
Native ($\lambda = 1.14000$) (SSRL)	20–3.8	282,088 26,257	99.7	10.0	
Os-MAD (Os peak: $\lambda = 1.1399$) (SSRL)	20–3.6	739,346 30,654	99.6	13.4	0.85
Os-MAD (high energy: $\lambda = 1.107$) (SSRL)	20–3.6	801,825 30,585	99.4	14.2	1.09/0.90
Figure of merit[c]: 0.22/0.21	20–3.6				
Native ($\lambda = 1.10000$) (NSLS/X-25)	20–2.7	552,088 60,657	83.0	13.6	
Os-SAD (Os peak: $\lambda = 1.1400$) (NSLS/X-25)	20–3.6	684,691 58,829	99.8	10.0	0.97/1.38
U ($\lambda = 1.13960$) (SSRL)	20–3.4	308,703 35,635	99.2	7.7	1.54
Os/U-SAD (low energy: $\lambda = 1.1396$) (SSRL)	20–3.5	297,881 57,791	97.7	6.7	1.54/1.63
Figure of merit[c]: 0.31/0.39	20–3.5				

Molecular Model Refinement:

Dataset	Resolution Å	Reflections (Measured/Unique)	Completeness	R_{sym}[a]
Native ($\lambda = 1.1000$) (NSLS/X-25)	20–2.7	552,088 60,657	83.0	13.6

Reflections	Number of Atoms	R_{free}[d] ($R_{working}$[e])	Rmsd (Å) Bonds	Rmsd (Å) Angles	Rmsd B Values (Å^2) (Main Chain)	(Side Chain)
49,155	13,828	30.38 (26.06)	0.00114	1.72	1.435	1.706

[a] $R_{sym} = 100 \times \Sigma|I - \langle I \rangle|/\Sigma I$, where I is the integrated intensity of a given reflection.
[b] Phasing power = $\Sigma|F_H|/\Sigma||F_{PH}(obs)| - |F_{PH}(calc)||$, where F_H is the calculated heavy atom structure factor amplitude.
[c] Figure of merit = $\langle|\Sigma P(\alpha)e^{i\alpha}/\Sigma|P(\alpha)|\rangle$, where α is the phase and $P(\alpha)$ is the phase probability distribution.
[d] $R_{free} = \Sigma|F(obs) - F(calc)|/\Sigma F(obs)$, calculated using 3.4% of the data.
[e] $R_{working} = \Sigma|F(obs) - F(calc)|/\Sigma F(obs)$.

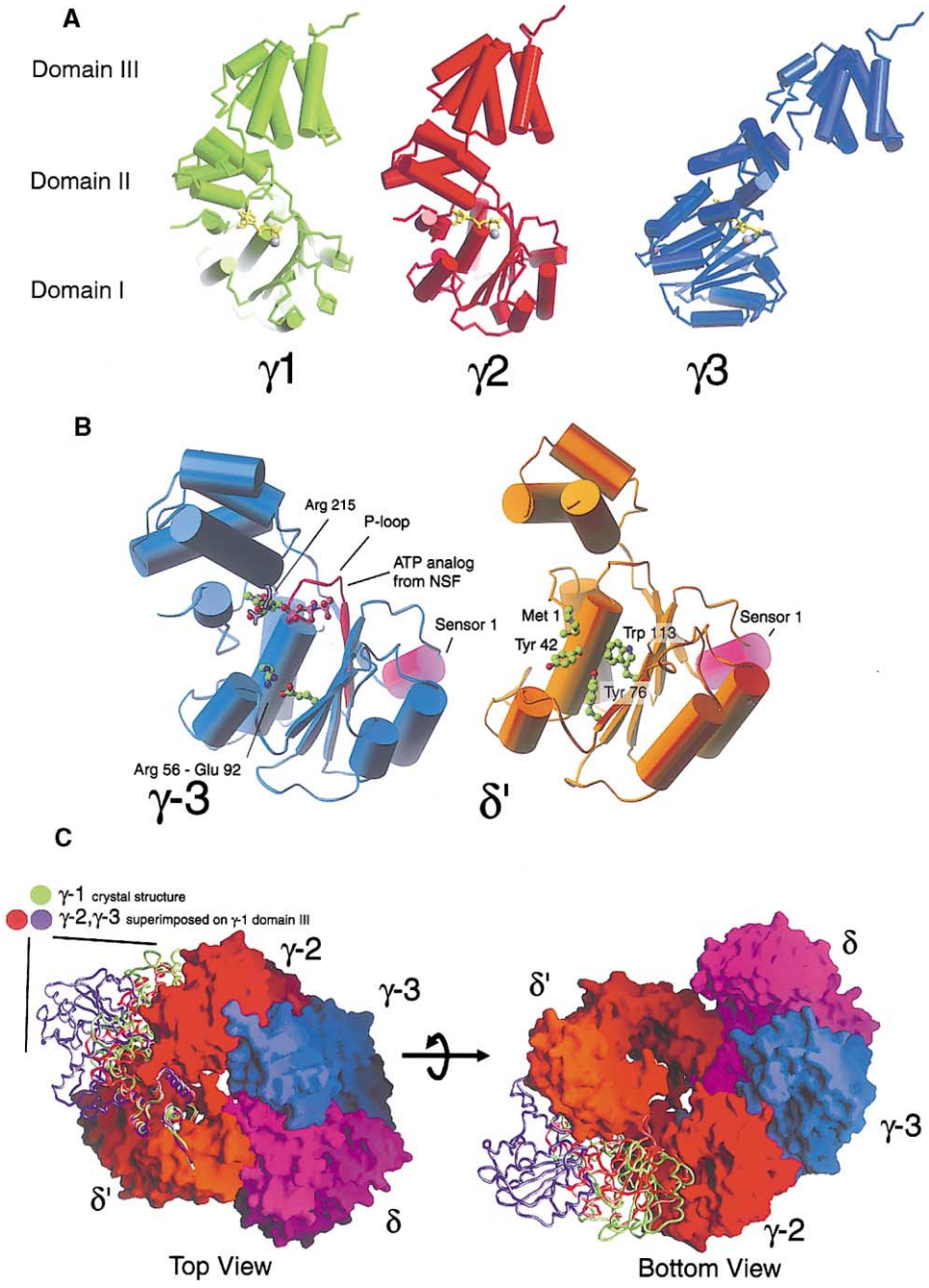

Figure 2. Structure of the γ Subunits

(A) Comparison of the structure of the three γ subunits after their C-terminal domains are overlaid. The ATP analog (yellow) is from NSF-D2 (PDB code 2D2N). See Figure 1 of the accompanying paper (Jeruzalmi et al., 2001) for the notation used for secondary structural elements.

(B) Comparison of the nucleotide binding site of γ3 with the equivalent region of δ′. Only Domains I and II are shown. The side chain of Arg-215 from the Sensor 2 region of γ is shown. Helix α6 in the Sensor 1 region is colored magenta. In δ′, the nucleotide binding site is blocked by the N-terminal extension, of which Met-1 is one of the residues forming a conserved hydrophobic patch on the surface (see Figure 5A). This hydrophobic patch is missing in γ, which has an ion pair at the position corresponding to Tyr-42 and Tyr-76. δ′ has a conserved Sensor 1 motif (magenta).

(C) Conformational changes in γ. The molecular surface of the γ complex is shown, except for γ1. The structure of γ1 is shown as a tube representing the backbone. The structures of γ2 and γ3 have been superimposed on that of γ1 using Domain III, and are also shown as tubes.

example, helix α9 is misaligned with the ATP binding site in such a way that the side chain of Arg-215 occupies the space where the ribose ring of the nucleotide is located in NSF-D2 and p97 (Figures 2 and 3A). Clearly, nucleotide binding would lead to a relocation of helix α9 such that Arg-215 can interact properly with the phosphate groups of ADP or ATP. Arg-215 is conserved in bacterial and eukaryotic clamp loaders, as well as in

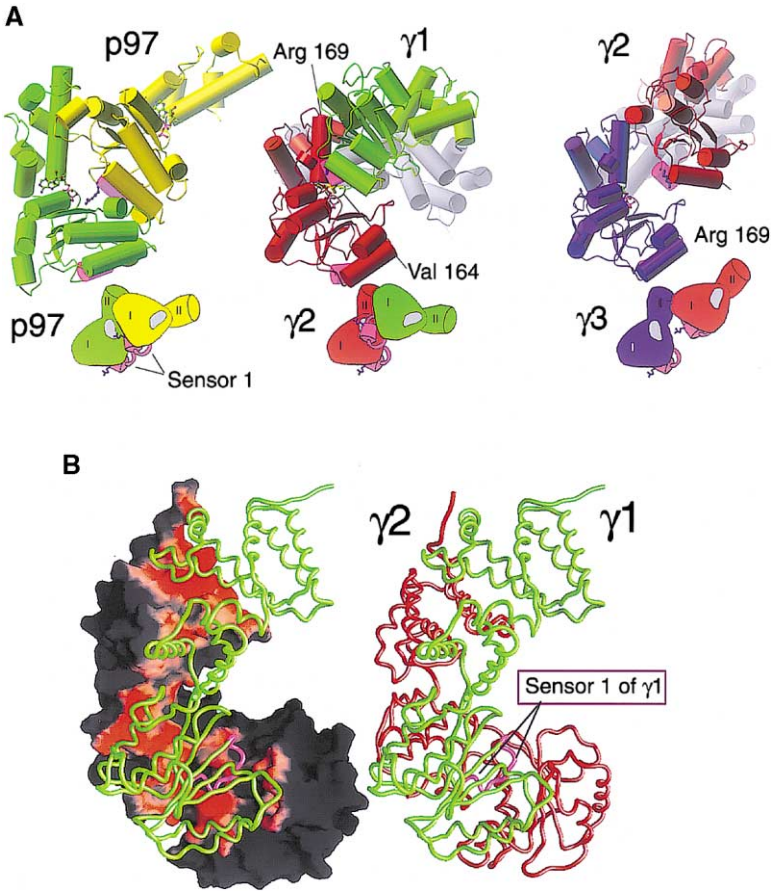

Figure 3. γ:γ Interfacial Nucleotide Binding Sites Compared to the NSF Homolog p97

(A) The nucleotide binding site of p97 (left) (Zhang et al., 2000) (PDB code 1E32) is compared to that of γ2 (at the γ1-γ2 interface, middle) and of γ3 (at the γ2-γ3 interface, right). For the γ structures, Domains I and II are colored, and Domain III is shown in gray. A schematic representation of the Domain I–II units is shown below the structures. ADP bound to p97 is shown at the active site of γ2 (middle) and γ3 (right) for reference. The arginine side chains of the Sensor 1 region are shown in dark blue at each interface.

(B) The Sensor 1 region of γ1 is buried at the γ1-γ2 interface. On the left, the γ1-γ2 pair of subunits is shown, with the molecular surface of γ2 colored in gray, highlighted in red where γ1 contacts the γ2 surface. γ1 is shown as a green tube representing the backbone, with the Sensor 1 region colored magenta. γ2 is shown with the surface removed on the right.

RFC subunits, where it is part of the conserved sequence motif (G/PxϕRxϕ, where ϕ denotes a hydrophobic residue) (Cullman et al., 1995).

The C-Terminal Domains of γ, δ, and δ′ Form a Helical Scaffold

The C-terminal domains of δ′ and the three γ subunits interact with each other in a similar manner (Figure 1C). Proceeding in the order δ′-γ1-γ2-γ3, the C-terminal helix α15 of the first subunit in a pair packs into a hydrophobic groove formed by helices α12 and α14 of the following subunit. The interface between the C-terminal domains is fairly extensive. For example, at the γ1-γ2 interface, 905 Å^2 and 937 Å^2 of surface area are buried on Domain III of the two subunits, respectively. There is tight packing of hydrophobic residues at each of the interfaces. In γ, these include Pro-343, Met-347, Met-351, Leu-354, Leu-357, and Leu-365 on one side of the interface, and Leu-286, Ala-293, Met-294, Leu-297, Tyr-329, and Leu-333 on the other side. In addition to the helical packing, flexible C-terminal extensions emanate from the domains, linking them together. These extensive interactions suggest that the C-terminal domains of δ′ and γ are linked together tightly and not easily perturbed.

The C-terminal domain of δ is bound between the corresponding domains of γ3 and δ′, closing the circle. However, the arrangement of the δ′ and γ subunits is such that there is not enough space to accommodate a fifth subunit that makes the same set of α15/α12–α14 interactions on both interacting faces (Figure 1D). Hence, the C-terminal domain of δ is displaced outward from the circle. On the side facing δ′, helices α12 and α14 of δ do interact with helix α15 of δ′, burying 862 Å^2 and 913 Å^2 of surface area on δ′ and δ, respectively. However, on the other side, helix α15 of δ interacts only peripherally with helix α12 and the loop following it in γ. The surface area buried at this interface is lower (461 Å^2 on γ3 and 440 Å^2 on δ), and is mainly polar rather than hydrophobic. Thus, the C-terminal domain of δ might swivel with respect to the rest of the helical scaffold as the γ complex undergoes conformational changes.

Interdomain Rotations Result in Large Structural Differences between the Three γ Subunits

The overall shape of each of the three γ subunits is different (Figure 2A). When viewed from above the C-terminal helical collar, the N-terminal domains of γ1, γ2, and γ3 are increasingly splayed out with respect to the roughly circular arrangement of the C-terminal domains, with Domain I of γ3 being rotated outward the most (Figure 2C). On superimposing Domain II, the relative rotation in Domain III is 21°, 45°, and 60° on comparing γ1 with γ2, γ2 with γ3, and γ1 with γ3, respectively. γ1 and γ2 are significantly closer to each other in overall structure than either is to γ3, a fact that is important in generating a model for a closed state of the γ complex, discussed later.

The relative changes in the Domain I/Domain II orientations are much smaller, and range from 4° (γ1/γ3) to 9° (γ1/γ3). The relative orientation of Domain I and Domain II in the nucleotide-free γ subunits is also close to that seen in NSF and other AAA+ ATPases bound to ATP and ADP (Lenzen et al., 1998; Yu et al., 1998) (Figure 3A). Thus, it seems that the role of Sensor 2 (in Domain II) may not be to induce large conformational changes in the γ subunit, but rather to stabilize the Domain I/II interface upon nucleotide binding. The very much larger conformational changes at the II/III interface underlie the ATP-driven transitions that drive clamp loading, and they appear to be controlled by the Sensor 1 switch and changes in the intersubunit packing, as discussed below.

Differences in the Structures of the γ Subunits Result in the Generation of Three Different Interfacial Nucleotide Binding Sites

Each of the nucleotide binding sites is in the vicinity of an interdomain interface (Figure 1C), and the general arrangement resembles that seen in the hexameric AAA+ ATPases, such as NSF (Figure 3). In NSF-D2 and p97, each monomer packs against the next one so that Domains I and II of the first monomer cradle Domain I of the next monomer (Figure 3A) (Lenzen et al., 1998; Yu et al., 1998; Zhang et al., 2000). This arrangement is such that the Sensor 1 region of the second monomer is positioned close to the P loop of the first monomer. In p97, the terminal atoms of the side chain of Arg-359 from the Sensor 1 helix of the second monomer are positioned ~4 Å from the β phosphate of ADP (Figure 3A) (Zhang et al., 2000). It is surmised that the role of this arginine is similar to that of the "arginine finger" utilized by GTPase-activating proteins to stimulate catalysis in their target GTP binding proteins (Ahmadian et al., 1997; Neuwald et al., 1999), thereby coupling changes in intersubunit packing to ATP hydrolysis. Arg-359 in p97 corresponds structurally to Arg-169 in helix α6 of γ, which is part of the conserved SRC motif in Sensor 1 of clamp loaders.

In each pair of subunits in the γ complex, the Sensor 1 region of the first subunit is positioned near the ATP binding site of the next one (Figure 3). Although δ′ does not bind nucleotides, it has the conserved Sensor 1 SRC motif, and this is positioned near the binding site of γ1. This arrangement is followed sequentially by γ1 and γ2 (Figure 3A). The Sensor 1 region of γ3 does not abut a nucleotide binding site since one is lacking in δ. Interestingly, Arg-169 from the SRC motif of γ3 is involved instead in a network of electrostatic and hydrophobic interactions that appears to bind Domains I and II of δ tightly to Domain I of γ3. The dual role of Arg-169, which acts as a potential "arginine finger" at three nucleotide binding sites and also serves to hold the δ subunit onto γ3, most likely accounts for the strict conservation of the SRC motif across evolution.

The nucleotide binding sites of γ1 (at the δ′-γ1 interface) and that of γ3 (at the γ2-γ3 interface) are both open, in that nucleotide binding is not impeded. However, comparison with the structures of NSF and p97 shows that the arginine of the SRC motifs in δ′ and γ2 are too far away to interact with the phosphates of ATP for catalysis (Figure 3A). At the γ1-γ2 interface, helix α6 in the Sensor 1 region of γ1 approaches the nucleotide binding site of γ2 closely, but it does so in a way that completely blocks nucleotide binding and misaligns Arg-169 (Figure 3A). We do not as yet understand the structural changes that are required for proper alignment of the Sensor 1 region with the ATP binding sites, particularly since the highly symmetric structures of other AAA+ ATPases contrast sharply with the asymmetric γ complex structure.

The Closed Interface between γ1 and γ2 Is Extensive, and Buries Sensor 1 of γ1 at its Center

There is an extensive interface between Domains I and II of γ1 and γ2 that leads to the burial of ~3,000 Å^2 at the interface (1,532 Å^2 on γ1, and 1,469 Å^2 on γ2), not including Domain III of either subunit. This is by far the most extensive interface between subunits in the γ complex. The interface is almost exclusively polar, and involves an extensive complementarity in shape between the two subunits (Figure 3B). Nucleotide binding at the γ2 binding site is impeded by helix α6 of the Sensor 1 region of γ1, which approaches closely and positions the side chain of Val-164 such that it blocks the phosphate binding site (Figure 3A).

The entire Sensor 1 region of γ1 is at the heart of this interface with γ2 (Figure 3B). As we discuss later, the nucleotide binding site of γ1, at the interface between δ′ and γ1, is likely to be constitutively open, and thus ATP binding to γ1 is not blocked as it is in γ2. By analogy to G proteins (Vetter and Wittinghofer, 1999), the Sensor 1 region is likely to respond exclusively to the binding of nucleotide triphosphates, and ATP binding (but not ADP binding) at the γ1 site is likely to alter the conformation of the Sensor 1 region of γ1. This can, in turn, disrupt the network of interactions around α6 in the γ1-γ2 interface. The almost exclusive polar nature of this interface suggests that the energetic cost of disrupting it may be compensated substantially by the resulting solvation of interfacial residues.

The ATP Binding Site of γ3, at the γ2-γ3 Interface, Is Open and Causes the δ Wrench to Be Swung Out

In contrast to the extensive and closed γ1-γ2 interface, the γ2-γ3 interface is wide open and involves minimal contacts between Domains I and II of the subunits (only 214 Å^2 and 261 Å^2 of surface area are buried on Domains I and II of γ2 and γ3, respectively, at this interface). The opening of the interface is due primarily to the rotation of Domains I and II of γ3 outward by ~45° with respect to their orientation in γ2 (Figure 3A).

The flexible linker between Domains II and III of the δ subunit allows Domains I and II of δ to move away from the body of the γ complex, while remaining associated with γ3 (806 Å^2 and 832 Å^2 of surface area buried on γ3 and δ, respectively, excluding Domain III). The interface primarily involves Domain I of γ3, which binds mainly to Domain II of δ. Hydrophobic interactions at the interface occur at two patches. One patch includes Leu-190 and Leu-191 from δ and Phe-173 and Ala-27 from γ. The other patch involves interactions between Leu-29 and Leu-179 from δ and Val-164 and Leu-167 from γ3, both of which are in the Sensor 1 region of γ3.

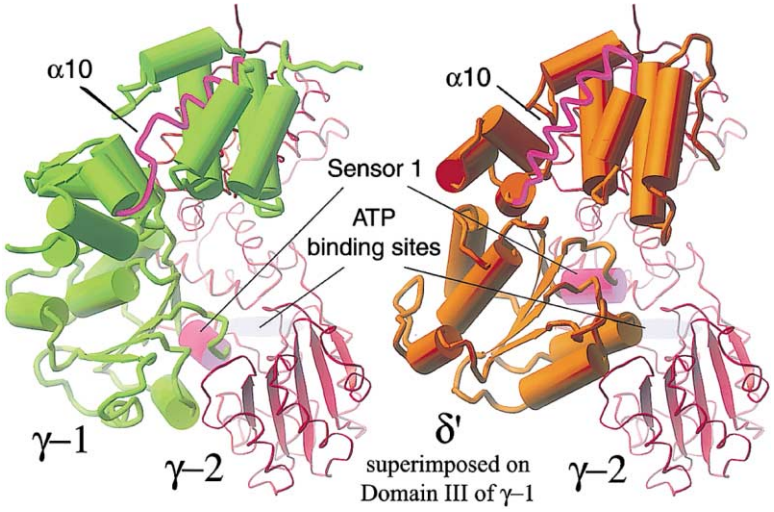

Figure 4. The δ′ Stator Is Unlikely to Cause Closure of the Adjacent γ1 ATP Binding Site

On the left, the γ1 (green) and γ2 (red) pair of subunits is shown, with Sensor 1 of γ1 (magenta) positioned near the ATP binding site of γ2 (indicated in gray). The first helix of Domain III of γ1, α10, is shown as a magenta tube to highlight the flexible linker connecting it to the last helix of Domain II. On the right, γ2 is shown again, in the same orientation as on the left (red). The γ1 subunit is replaced by δ′ (orange), which has been superimposed on γ1 using the C-terminal domain. Note that helix α10 in δ′ is extended at its N terminus relative to the structure seen in γ1, so that the connection to Domain II no longer appears to be flexible. The overall conformation of δ′ is more closed than that of γ1, so that the Sensor 1 region of δ′ is no longer located as close to the ATP binding site of γ2 as that of γ1.

Arg-169 of the Sensor 1 motif of γ3 participates in a network of electrostatic interactions involving Asp-36 and Gln-32 of δ.

Rigidity in the Structure of the δ′ Stator Is Likely to Hold the δ′-γ1 Interface Open

The ATP binding site of γ1, at the δ′-γ1 interface, is open and involves minimal interactions between Domains I and II of these subunits (surface area buried on Domains I and II is 352 Å^2 on δ′ and 340 Å^2 on γ2, excluding Domain III). While the γ-γ interfaces can clearly exist in open and closed states, the δ′-γ1 interface is likely to be held open constitutively. A critical aspect of the closure of the ATP binding site of γ2, at the γ1-γ2 interface, is a difference in the orientation of Domain II in γ1 when compared to δ′. This change moves the Sensor 1 region from the vicinity of Domain II (where δ′ places it on γ1) to a location where it fits into the nucleotide binding site on γ2 (see Figure 4).

The conformation adopted by γ1 appears to be prevented in δ′ by the lack of a flexible linker between Domain II and Domain III. The residues that in γ allow a wide range of motion between Domains II and III are part of an extended helix α10 in δ′, with a single residue connection between this helix and helix α9 in Domain II (Figure 4). In addition, the presence of hydrophobic interactions at the II-III interdomain interface in δ′ appears to further limit conformational changes at the interface. The relatively closed "C" shape of δ′ in isolation (Guenther et al., 1997) is maintained in the crystal structure of the γ complex.

Implications for Structural Transitions in the γ Complex

The particular conformation seen here for the γ complex is most likely a consequence of crystal packing interactions that hold δ′ and δ apart. Biochemical experiments demonstrate that the γ complex undergoes ATP-dependent transitions that either sequester or expose δ for interaction with the β ring (Naktinis et al., 1995), and that the δ′ subunit is involved in this sequestration (Turner et al., 1999). Since the crystal structure has Domain I of δ almost completely exposed, we asked whether we could alter the structure in a simple way that would result in an interaction between the N-terminal domains of δ and δ′. The results of a crude modeling exercise that does this is presented in the next section. The next two sections discuss the docking of the β subunit onto the γ complex.

Conformational changes in human RFC as a result of binding to ATP and to the PCNA clamp have been studied at low resolution (Shiomi et al., 2000). In the absence of ATP, the RFC complex adopts a closed circular or oval structure, described as a closed "U." In the presence of ATP, this converts to a more open "C"-shaped form. While the low resolution of the electron microscopic analysis makes direct comparisons difficult, it appears that the ATP-free closed U form is similar to our model for the closed form of δ (Figure 5A). The open C-shaped form resembles the crystal structure or the slightly modified form of it that is docked to the β ring (Figure 5C). The positions of the N-terminal domains of γ3 and δ relative to the C-terminal domains in the γ complex are reminiscent of a splayed-out structure seen in NSF in the presence of ATP (Hanson et al., 1997).

Closure of the Open ATP Site of γ2 at the γ2-γ3 Interface Results in the β-Interacting Element of δ Being Bound to δ′

We generated a crude model for a closed form of the γ complex by first replicating the γ1-γ2 pair of subunits and then superimposing the C-terminal domain of γ1 on that of γ2 in the crystal structure. This "ratchets" the γ1-γ2 pair by one position along the helical collar, and the transformed γ2 model was considered to be the new conformation of γ3. Once this was done, Domains I and II of δ were moved as a rigid body so that their orientation relative to the new position of the N-terminal domain of γ3 is precisely the same as that seen in the crystal structure of the γ complex. In effect, the N-terminal domain of γ3 moves as a rigidly coupled unit to Domains I and II of δ as γ3 closes upon γ2 (Figure 5A).

Our rather crude model for a potential closed form of the γ complex explains the low affinity of nucleotide-free γ complex for the β subunit. When γ3 closes upon γ2, the tracking of this movement by Domains I and II

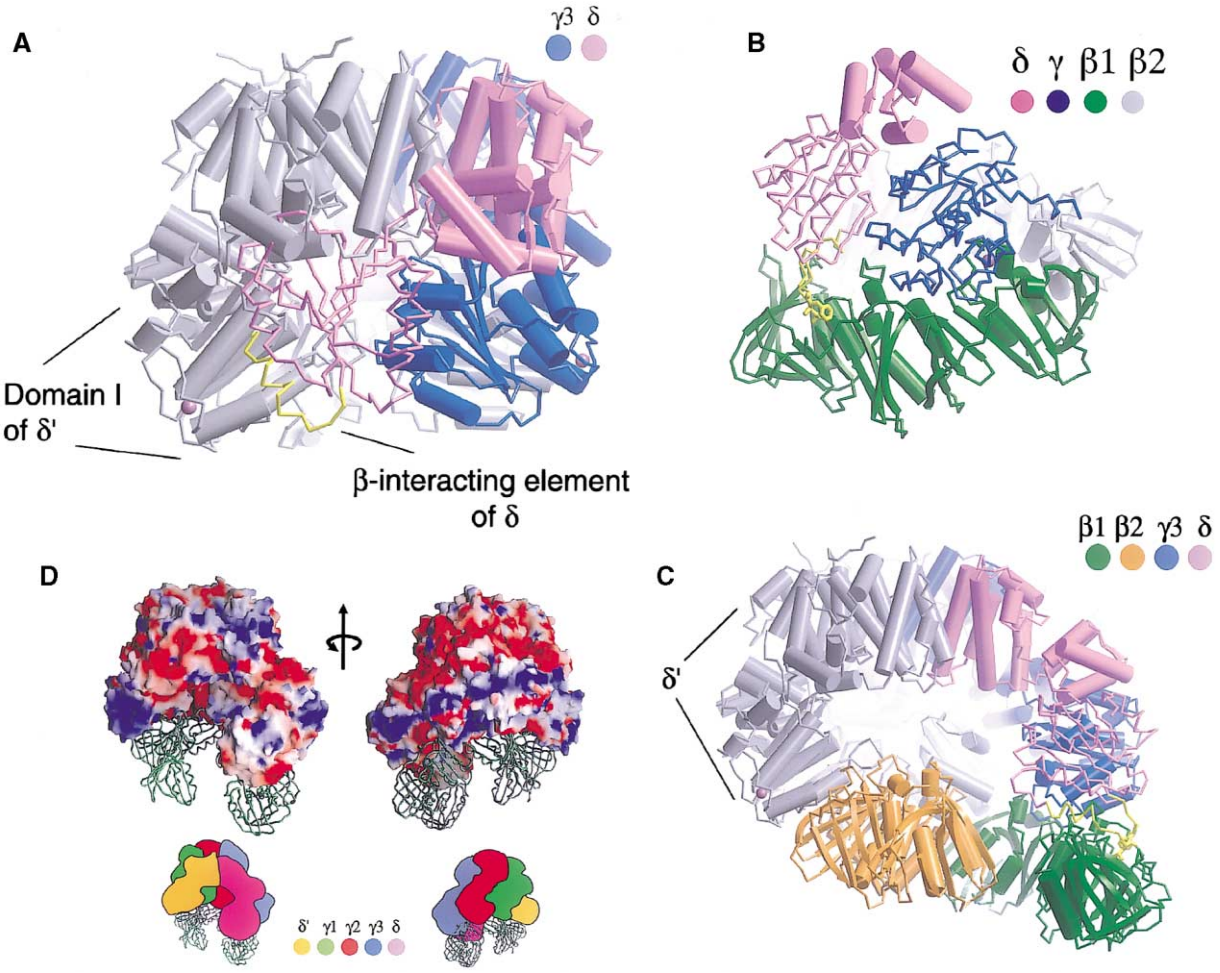

Figure 5. Model for the Open and Closed (Nucleotide-Free Conformation) of the γ Complex

(A) The γ1-γ2 pair of subunits in the crystal structure was replicated and moved forward by one position in the assembly by superimposing the C-terminal domain of γ1 in the new γ1-γ2 pair on that of γ2 in the crystal structure. The transformed γ2 is shown here in the position corresponding to γ3 (blue). Domains I and II of δ (magenta) were moved as a rigid body so as to preserve their relative orientation with respect to Domain I of γ3. The edge of Domain I of δ interacts with the face of δ′ such that the β-interacting element (yellow) packs against the hydrophobic patch on the δ′ surface (see Figure 2B). The clash between the edge of Domain I of δ and the δ′ subunit could be relieved by small adjustments in other subunits, but this has not been modeled.

(B) Model for a dimeric open form of the β clamp docked onto the γ complex. A δ-γ3 subassembly containing Domains I and II of δ and Domain I of γ3 (from the γ complex structure) was docked onto the surface of β based on the β:δ structure. The figure shows the structure of the model for the open form of the ring in green and gray, the δ subunit in magenta, and γ3 in blue. The structure of the N-terminal domain of δ (shown as a thin tube) corresponds to that in the β:δ complex, while the structure of Domain II of δ and Domain I of γ3 is from the γ complex.

(C) The γ complex, colored in gray except for δ (magenta) and γ3 (blue), is shown docked to the open form of the β ring, generated as described in the accompanying paper (Jeruzalmi et al., 2001). The only adjustment in the γ complex relative to the crystal structure is in the δ-γ3 subassembly containing Domains I and II of δ and Domain I of γ3, which was rotated outward by ~30° as a rigid body, along with the β ring.

(D) Two views of the docked β subunit and the γ complex, rotated by 180° about a vertical axis. The electrostatic potential at the molecular surface is shown, colored from red (negative) to blue (positive). Calculated and displayed using GRASP (Nicholls et al., 1991).

of δ results in the β-interacting element of δ (helix α4) landing on the surface of the N-terminal domain of δ′, close to what would be the nucleotide binding site in γ (Figure 5A). The resultant packing between δ and δ′ is not perfect: it involves collisions between the edge of Domain I of δ and the face of δ′, but these can readily be resolved by slight adjustment in the various domains, which we have not attempted.

The β-interacting element on δ undergoes a very significant conformational change upon binding to β, as discussed in the accompanying paper (Jeruzalmi et al., 2001). Helix α4 in the β:δ complex is partially unwound, rotated, and translocated in order to expose the two hydrophobic residues (Leu-73 and Phe-74) that are critical for the anchoring of δ on the β surface. In the conformation of δ seen in the crystal structure of the γ complex, Leu-73 and Phe-74 are withdrawn onto to the surface of δ, and two other hydrophobic side chains, Trp-61 and Phe-62 are exposed (see Figure 4C in the accompanying paper, Jeruzalmi et al., 2001). The model for the closed

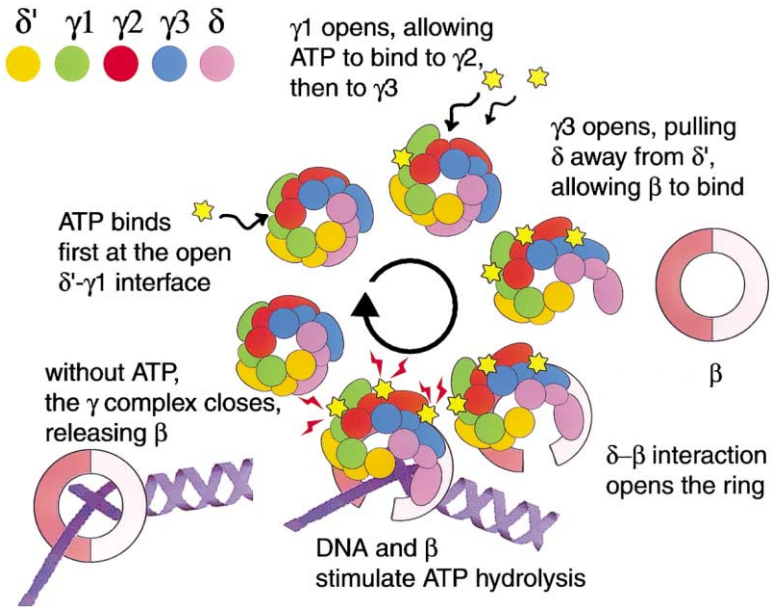

Figure 6. Schematic diagram of the clamp loading cycle

A cartoon of the reaction cycle performed by the clamp loader, based on a combination of biochemical data (see, for example, Turner et al., 1999) and structural information presented in this paper and the accompanying one.

form of the γ complex causes the burial of Trp-61 and Phe-62 of δ in an exposed hydrophobic groove on the surface of δ′. This groove is formed by the surface of the central β sheet of the N-terminal domain of δ′, and is bordered by helix α2 (Figure 2B).

The δ-γ3 Subassembly of the γ Complex Is Structured so that γ3 Can Mimic the β:δ Interaction at an Adjoining Intersubunit Region on β

We used the crystal structure of the β:δ complex to dock the N-terminal domain of δ, as well as the β subunit, from that structure onto the δ subunit in the γ complex. When this is done, a very interesting correlation between the structure of the β subunit and the structure of the δ-γ3 subassembly is evident. In the docked complex, the N-terminal domain of γ3 interacts with the surface of β in a manner that resembles the interaction of δ with β (Figure 5B). Helix α4 of γ approaches the surface of β closely at the interdomain interface between Domains 1 and 2 and near the interdomain connector. δ interacts with β similarly, using helix α4, but at the interface between Domains 2 and 3. The lack of significant steric clash between the δ-γ3 subassembly and the almost precise mimicking by γ of the δ-β interaction suggests a role for γ in binding to the clamp. Recent biochemical data support this idea (Stewart et al., 2001).

Adjustments in the Orientation of the δ-γ3 Subassembly Allow Docking of an Open Form of the Entire β Ring on the Surface of the Clamp Loader

Docking of β onto the unmodified crystal structure of the γ complex, using δ in the β:δ complex as a reference, results in a collision between γ2, γ1, and δ′ and the β dimer. We relieved these collisions by generating a crude model for an open form of β docked onto the surface of the clamp loader. We separated the clamp loader and the β dimer into two parts that were treated as rigid bodies in a docking calculation. The δ-γ3 subassembly (Domains I and II of δ and Domain I of γ3), along with the β dimer, was treated as one rigid body, and everything else as a second rigid body. The δ-γ3 subassembly was docked onto the surface of the open form of the β dimer, generated from the crystal structure of the β:δ complex (Figure 4D of the accompanying paper, Jeruzalmi et al., 2001). This docking results in no serious interpenetration of structures, as discussed in the previous section (Figure 5B). The δ-γ3-β_2 assembly was then moved away from the rest of the γ complex and then docked onto it using a rigid body procedure that considered only van der Waals repulsions between backbone atoms, along with harmonic forces on the Cα atoms of the clamp loader that restrained them to be close to the crystal structure. The restraint term was set to be maximal (300 kcal/mole/Å^2) at the connection points between Domains II and III of δ and between Domains I and II of γ3, and it was reduced as the inverse square of the distance from these pivot points. An ~30° outward rotation of the δ-γ3 subassembly allows docking of the entire open form of the β dimer on the surface of the clamp loader (Figure 5C). This very simplistic modeling procedure ignores conformational changes within the γ complex and results in localized intermolecular clashes, which are ignored.

The model for the γ complex bound to β makes clear that the orientation of the β:δ interaction virtually dictates that an extensive interaction will occur between β and the various subunits of the γ complex, including δ′. The multipoint interaction between β and the clamp loader that is suggested by this analysis has important implications for the clamp loading process because it potentially provides a way for the clamp loader to stabilize the ring while allowing one interface to open. For example, in the RFC/PCNA system, the interaction between the subunit corresponding to γ3 and PCNA would occur at an intermolecular interface, but one that is presumably being stabilized rather than being opened.

Calculation of the surface electrostatic potential of the γ complex using GRASP (Nicholls et al., 1991) reveals

two extensive regions of positive electrostatic potential. One region is located on the δ subunit, directly above the hole in the β subunit, and provides a direct pathway for DNA to transit into the ring while interacting with the γ complex. Intriguingly, there is a fairly contiguous belt of positive electrostatic potential that runs along the outer surface of the N-terminal domains of the γ complex (Figure 5D). If double-stranded DNA is cradled within the open β dimer, it is possible that the interaction of single-stranded DNA with the outer surfaces of the ATP binding domains might provide a mechanism for the rearrangement of the Sensor 2 elements such that ATP hydrolysis is stimulated.

Conclusion

We can integrate the wealth of biochemical data regarding the clamp loading process with the new structural information into a model for the clamp loading cycle (Figure 6). While speculative, this model provides a useful basis for designing new experiments to further probe the mechanism of clamp loader action in the *E. coli* and other systems.

In the absence of ATP, we assume that the two γ-γ interfaces in the clamp loader are both closed, adopting conformations similar to that seen in the γ1-γ2 interface in the crystal structure. This would result in the closure of the δ-δ′ interface, as shown in Figure 5A, preventing δ from interacting with β. δ′ appears to be the stator in the clamp loader motor, staying relatively rigid throughout the cycle. This causes the δ′-γ1 interface to stay open, allowing ATP access to the nucleotide binding site of γ1, where it can trigger structural changes in the Sensor 1 region of the γ1 subunit. It is expected that the Sensor 1 switch in the clamp loaders and the AAA+ ATPases functions similarly to the Switch 2 region of G proteins, which responds specifically to nucleotide triphosphates. Thus, ATP, and not ADP, is required to trigger a change in the Sensor 1 region of γ1.

The closed γ1-γ2 interface (the γ2 ATP binding site) buries at its center the Sensor 1 region of γ1. ATP binding to γ1 will alter the conformation of its Sensor 1 element, perhaps causing γ1 to fall away from γ2 and becoming loosely pendant (as is γ3 in the crystal structure). This would allow ATP to now bind to γ2, thereby disrupting the γ2-γ3 interface in turn. We surmise that the release of the γ3 subunit causes it to swing out from the body of the γ complex, as observed in the crystal structure. This moves δ away from δ′, and allows the N-terminal domains of the clamp loader to interact with β, anchored by δ.

A minimum of one ATP binding event (at the δ′-γ1 interface) is required to initiate this series of conformational changes. Data for the *E. coli* system suggest that 2–3 ATP molecules are hydrolyzed by the clamp loader in each cycle (Turner et al., 1999) (Bertram et al., 2000), and recent data on the T4 system indicate that one ATP molecule is minimally required for clamp loading (Pietroni et al., 2001). The low basal ATPase activity of the γ complex is actually suppressed by the presence of β (Turner et al., 1999), suggesting that although the clamp-bound form of the γ complex has ATP bound to it, it does not have the Sensor 1 regions properly configured for catalysis. The addition of primed DNA stimulates the ATPase activity of the γ complex ~100 fold (Onrust et al., 1991), and the analysis of the structural changes induced in the γ complex by the simultaneous presence of the β clamp and DNA is an exciting avenue for future investigations. Once ATP is hydrolyzed, we surmise that the binding energy of ADP is insufficient to prevent the γ-γ interfaces from closing again, thereby resetting the system and releasing β onto DNA (Hingorani and O'Donnell, 1998; Turner et al., 1999).

A key inference from our proposed mechanism is that the role of ATP binding is not to force the γ complex into a defined ATP-dependent conformation that then interacts with and pulls apart the ring. Rather, we propose that ATP is required for the disruption of the closed conformation of the γ complex, which then unleashes the hydrophobic β-interacting element of the δ subunit on a flexibly linked tether. The hydrophobic interaction between the δ wrench and β opens the β ring not by physically prying it open, but by stabilizing a conformation of β that is inconsistent with ring closure. Most members of the AAA+ ATPase superfamily, of which the γ complex and RFC subunits are members, are involved in the dismantling or restructuring of supramolecular assemblies of proteins (May et al., 2001). It is possible that the ATP-dependent exposure of flexible domains with hydrophobic interaction elements will prove to be a common aspect of the mechanism of action of AAA+ ATPases.

Experimental Procedures

Sample Preparation and Characterization

The γ, δ, and δ′ subunits of *E. coli* DNA polymerase III were purified and the γ complex was reconstituted as described (Turner et al., 1999). Limited proteolysis of the γ complex using elastase revealed that the C-terminal 6 kDa of the γ subunit was labile, while δ and δ′ were relatively stable. Truncated γ subunit (residues 1 to 373) was overexpressed as a glutathione S-transferase fusion protein, and purified over glutathione sepharose, followed by release of the γ subunit using the tobacco etch virus (TEV) protease. Isolated γ subunit was flowed over glutathione sepharose and sulphopropyl sepharose to resolve it from uncleaved protein, released glutathione S-transferase, and TEV protease. A final chromatographic step over Source Q yielded 97%–98% pure truncated γ subunit, which was reconstituted into γ complex as for the wild-type complex and purified over Source Q. Activity assays indicated that this γ complex was fully active as a clamp loader (data not shown). Multiangle laser light scattering (Wyatt Technologies) indicated that the γ complex was monodisperse in solution, and the data were consistent with a molecular weight of 195 kDa, consistent with the predicted molecular mass of 200 kDa for a $\gamma_3\delta\delta'$ assembly.

Crystallization and X-Ray Crystallography

The γ complex was prepared for crystallization trials by dialysis against 20 mM TRIS-HCl, pH 7.5, 2 mM dithiothreitol, and concentrated to 100 mg/ml by ultrafiltration (Millipore). Crystals of γ complex were grown from solutions containing 100 mg/ml $\gamma_3\delta\delta'$, 50 mM HEPES, pH 7.5, 1.05–1.15 M ammonium sulfate, 6%–7.5% polyethylene-glycol 400, 320 mM N,N-dimethylacetamide, 4 mM dithiothreitol. The crystals are in orthorhombic space group $P2_12_12_1$, with cell parameters a = 95.7 Å, b = 95.9 Å, c = 285.4 Å, and one γ complex in the asymmetric unit. The a and b unit cell edges are coincidentally close to identical. While this initially caused significant confusion, the diffraction data show no evidence of tetragonal symmetry or twinning, and the molecular packing of the solved crystal structure reveals no obvious relationship to tetragonal packing. Diffraction data to 2.7/3.0 Å were measured from crystals cryoprotected in crystallization medium supplemented with 25% glycerol, at −180°C, using synchrotron radiation (Table 1).

Structure Determination, Model Refinement, and Analysis

The crystal structure of the γ complex was determined by a combination of multiple isomorphous replacement and anomalous dispersion methods. A tantalum bromide cluster yielded phasing information to 3.5 Å (Cramer et al., 2000; Seth Darst, personal communication), which was combined with phases from other isomorphous derivatives (Table 1). There are subtle differences between some data sets collected at various synchrotrons that prevented combination of derivatives into one phase set, and so the derivative data sets are divided into five groups in a joint phase calculation using MLPHARE (Collaborative Computational Project, 1994) and SHARP (La Fortelle and Bricogne, 1997). The five phase sets (Table 1) were treated as separate crystal forms in multicrystal noncrystallographic symmetry averaging calculation (DMMULTI) (Collaborative Computational Project, 1994), where each clamp loader subunit was treated as three separate domains. This procedure allowed a 3.0 Å map to be calculated of sufficient quality to allow accurate positioning of the backbone and fitting of amino acid side chain information. Attempts to average electron densities corresponding to the three γ subunits failed to improve the maps.

The molecular model of the γ complex was refined against data extending to 2.7/3.0 Å, using ONO and CNS (Brunger et al., 1998; Kleywegt and Jones, 1996). Refinement was performed against the residual and maximum likelihood (MLF) targets in CNS, along with use of experimental phase information (MLHL). The final model contains residues 3 to 368 of γ1, γ2, and γ3, as well as a zinc atom and a sulfate group in each γ subunit, residues 1–326 of δ′, and a zinc atom, and residues 1–334 of δ. No water molecules are modeled. We could position amino acid side chains with confidence, except for the very C-terminal region of the γ subunits (residues 363–373), the C terminus of δ′ (residues 325–334), and several regions in the C-terminal domain of δ (residues 314–321 and 334–343). The final models display working and free R values against the experimental data of 26.1% and 30.4%, respectively. The final model shows no outliers in the Ramachandran plot. Coordinates have been deposited with the Protein Data Bank under the accession code 1JR3.

Acknowledgments

We are grateful to members of the Kuriyan lab for stimulating discussions and for assistance in the measurement of diffraction data. We wish to thank S. Darst for sharing methods and code for handling heavy metal clusters in crystallographic phasing calculations, J. Turner, N. Yao, and F. Leu for engaging scientific discussions, M. Uy for technical assistance, and L. Leighton for help with illustrations. We thank Gunter Schneider for sharing unlimited quantities of Ta_6Br_{12} along with its crystal structure. We are indebted to the scientific staffs of the Advanced Light Source, the Cornell High Energy Synchrotron Source, the National Synchrotron Light Source, the Stanford Synchrotron Radiation Laboratory, and the Structural Biology Center at the Advanced Photon Source for assistance in the collection of diffraction data. Protein and DNA sequencing was performed by the Protein/DNA Technology Center of the Rockefeller University. Partial support for this work was provided by NIH grants GM RO1-45547 (J.K.) and GM RO1-38839 (M.O.D.).

Received June 25, 2001; revised July 20, 2001.

References

Ahmadian, M.R., Stege, P., Scheffzek, K., and Wittinghofer, A. (1997). Confirmation of the arginine-finger hypothesis for the GAP-stimulated GTP-hydrolysis reaction of Ras. Nat. Struct. Biol. *4*, 686–689.

Alberts, B.M., Barry, J., Bedinger, P., Formosa, T., Jongeneel, C.V., and Kreuzer, K.N. (1983). Studies on DNA replication in the bacteriophage T4 in vitro system. Cold Spring Harb. Symp. Quant. Biol. *47*, 655–668.

Bertram, J.G., Bloom, L.B., Hingorani, M.M., Beechem, J.M., O'Donnell, M., and Goodman, M.F. (2000). Molecular mechanism and energetics of clamp assembly in Escherichia coli. The role of ATP hydrolysis when gamma complex loads beta on DNA. J. Biol. Chem. *275*, 28413–28420.

Brunger, A.T., Adams, P.D., Clore, G.M., DeLano, W.L., Gros, P., Grosse-Kunstleve, R.W., Jiang, J.S., Kuszewski, J., Nilges, M., and Pannu, N.S. (1998). Crystallography & NMR system: A new software suite for macromolecular structure determination. Acta Crystallogr. D Biol. Crystallogr. *54*, 905–921.

Collaborative Computational Project, Number 4. (1994). The CCP4 suite programs for protein crystallography. Acta Crystallogr. D *50*, 760–763.

Cramer, P., Bushnell, D.A., Fu, J., Gnatt, A.L., Maier-Davis, B., Thompson, N.E., Burgess, R.R., Edwards, A.M., David, P.R., and Kornberg, R.D. (2000). Architecture of RNA polymerase II and implications for the transcription mechanism. Science *288*, 640–649.

Cullman, G., Fien, K., Kobayashi, R., and Stillman, B. (1995). Characterization of the five replication factor C genes of *Saccharomyces cerevisiae*. Mol. Cell. Biol. *15*, 4661–4671.

Flower, A.M., and McHenry, C.S. (1990). The γ subunit of DNA polymerase III holoenzyme of *Escherichia coli* is produced by ribosomal frameshifting. Proc. Natl. Acad. Sci. USA *87*, 3713–3717.

Guenther, B.D., Onrust, R., Sali, A., O'Donnell, M., and Kuriyan, J. (1997). Crystal structure of the δ′ subunit of the clamp-loader complex of E. coli DNA polymerase III. Cell *91*, 335–345.

Gulbis, J.M., Kelman, Z., Hurwitz, J., O'Donnell, M., and Kuriyan, J. (1996). Structure of the C-terminal region of $p21^{waf1/cip1}$ complexed with human PCNA. Cell *87*, 297–306.

Hanson, P.I., Roth, R., Morisaki, H., Jahn, R., and Heuser, J.E. (1997). Structure and conformational changes in NSF and its membrane receptor complexes visualized by quick-freeze/deep-etch electron microscopy. Cell *90*, 523–535.

Hingorani, M.M., and O'Donnell, M. (1998). ATP binding to the Escherichia coli clamp loader powers opening of the ring-shaped clamp of DNA polymerase III holoenzyme. J. Biol. Chem. *273*, 24550–24563.

Hingorani, M.M., and O'Donnell, M. (2000). Sliding clamps: a (tail)ored fit. Curr. Biol. *10*, R25–R29.

Kelman, Z., and O'Donnell, M. (1995). DNA polymerase III holoenzyme: Structure and function of a chromosomal replicating machine. Annu. Rev. Biochem. *64*, 171–200.

Kim, S., Dallman, H.G., McHenry, C.S., and Marians, K.J. (1996). Tau couples the leading- and lagging-strand polymerases at the Escherichia coli DNA replication fork. J. Biol. Chem. *271*, 21406–21412.

Kleywegt, G.J., and Jones, T.A. (1996). Efficient rebuilding of protein structures. Acta Crystallogr. D *50*, 829–832.

Kong, X.P., Onrust, R., O'Donnell, M., and Kuriyan, J. (1992). Three-dimensional structure of the beta subunit of E. coli DNA polymerase III holoenzyme: a sliding DNA clamp. Cell *69*, 425–437.

Krishna, T.S.R., Kong, X.-P., Gary, S., Burgers, P., and Kuriyan, J. (1994). Crystal structure of the eukaryotic DNA polymerase processivity factor PCNA. Cell *79*, 1233–1243.

La Fortelle, E.D., and Bricogne, G. (1997). Maximum-likelihood heavy-atom parameter refinement in the MIR and MAD methods. Methods Enzymol. *276*, 472–494.

Lenzen, C.U., Steinmann, D., Whiteheart, S.W., and Weis, W.I. (1998). Crystal structure of the hexamerization domain of N-ethylmaleimide-sensitive fusion protein. Cell *94*, 525–536.

Liu, J., Smith, C.L., DeRyckere, D., DeAngelis, K., Martin, G.S., and Berger, J.M. (2000). Structure and function of Cdc6/Cdc18: implications for origin recognition and checkpoint control. Mol. Cell *6*, 637–648.

May, A.P., Whiteheart, S.W., and Weis, W.I. (2001). Unraveling the mechanism of the vesicle transport ATPase NSF, the N-ethylmaleimide-sensitive factor. J. Biol. Chem. *276*, 21991–21994.

McHenry, C.S. (1982). Purification and characterization of DNA polymerase III′. Identification of tau as a subunit of the DNA polymerase III holoenzyme. J. Biol. Chem. *257*, 2657–2663.

Moarefi, I., Jeruzalmi, D., Turner, J., O'Donnell, M., and Kuriyan, J. (2000). Crystal structure of the DNA polymerase processivity factor of T4 bacteriophage. J. Mol. Biol. *296*, 1215–1223.

Naktinis, V., Onrust, R., Fang, L., and O'Donnell, M. (1995). Assembly of a chromosomal replication machine: two DNA polymerases, a clamp loader, and sliding clamps in one holoenzyme particle. II.

Intermediate complex between the clamp loader and its clamp. J. Biol. Chem. *270*, 13358–13365.

Naktinis, V., Turner, J., and O'Donnell, M. (1996). A molecular switch in a replication machine defined by an internal competition for Protein Rings. Cell *84*, 137–145.

Neuwald, A.F., Aravind, L., Spouge, J.L., and Koonin, E.V. (1999). AAA+: A class of chaperone-like ATPases associated with the assembly, operation, and disassembly of protein complexes. Genome Res. *9*, 27–43.

Nicholls, A., Sharp, K.A., and Honig, B. (1991). Protein folding and association: insights from the interfacial and thermodynamic properties of hydrocarbons. Proteins Struct. Funct. Genet. *11*, 281–296.

O'Donnell, M.E. (1987). Accessory proteins bind a primed template and mediate rapid cycling of DNA polymerase III holoenzyme from Escherichia coli. J. Biol. Chem. *262*, 16558–16565.

O'Donnell, M., Onrust, R., Dean, F.B., Chen, M., and Hurwitz, J. (1993). Homology in accessory proteins of replicative polymerases - *E. coli* to humans. Nucleic Acids Res. *21*, 1–3.

Onrust, R., Finklestein, J., Naktinis, V., and O'Donnell, M. (1995a). Assembly of a chromosomal replication machine: two DNA polymerases, a clamp loader, and sliding clamps in one holoenzyme particle. I. Organization of the clamp loader. J. Biol. Chem. *270*, 13366–13377.

Onrust, R., Finklestein, J., Nakatinis, V., Turner, J., Fang, L., and O'Donnell, M. (1995b). Assembly of a chromosomal replication machine: two DNA polymerases, a clamp loader, and sliding clamps in one holoenzyme particle. III. Interface between two polymerases and the clamp loader. J. Biol. Chem. *270*, 13348–13357.

Onrust, R., Stukenberg, P.T., and O'Donnell, M. (1991). Analysis of the ATPase subassembly which initiates processive DNA synthesis by DNA polymerase. J. Biol. Chem. *266*, 21681–21686.

Oyama, T., Ishino, Y., Cann, I.K.O., Ishino, S., and Morikawa, K. (2001). Atomic sturcture of the clamp loader small subunit from *Pyrococcus furiosus*. Mol. Cell *8*, in press.

Pietroni, P., Young, M.C., Latham, G.J., and von Hippel, P.H. (2001). Dissection of the atp-driven reaction cycle of the bacteriophage t4 dna replication processivity clamp loading system. J. Mol. Biol. *309*, 869–891.

Pritchard, A.E., Dallmann, H.G., Glover, B.P., and McHenry, C.S. (2000). A novel assembly mechanism for the DNA polymerase III holoenzyme DnaX complex: association of δδ′ with DnaX(4) forms DnaX(3) δδ′. EMBO J. *19*, 6536–6545.

Shamoo, Y., and Steitz, T.A. (1999). Building a replisome from interacting pieces: sliding clamp complexed to a peptide from DNA polymerase and a polymerase editing complex. Cell *99*, 155–166.

Shiomi, Y., Usukura, J., Masamura, Y., Takeyasu, K., Nakayama, Y., Obuse, C., Yoshikawa, H., and Tsurimoto, T. (2000). ATP-dependent structural change of the eukaryotic clamp-loader protein, replication factor C. Proc. Natl. Acad. Sci. USA *97*, 14127–14132.

Stewart, J., Hingorani, M.M., Kelman, Z., and O'Donnell, M. (2001). Mechanism of beta clamp opening by the delta subunit of escherichia coli DNA polymerase III holoenzyme. J. Biol. Chem. *276*, 19182–19189.

Stillman, B. (1994). Smart machines at the DNA replication fork. Cell *78*, 725–728.

Studwell-Vaughan, P.S., and O'Donnell, M. (1991). Constitution of the twin polymerase of DNA polymerase III holoenzyme. J. Biol. Chem. *266*, 19833–19841.

Stukenberg, P.T., Studwell-Vaughan, P.S., and O'Donnell, M. (1991). Mechanism of the Sliding β−clamp of DNA Polymerase III Holoenzyme. J. Biol. Chem. *266*, 11328–11334.

Stukenberg, P.T., Turner, J., and O'Donnell, M. (1994). An explanation for lagging strand replication: polymerase hopping among DNA sliding clamps. Cell *78*, 877–887.

Tsuchihashi, Z., and Kornberg, A. (1990). Translational frameshifting generates the γ subunit of DNA polymerase III holoenzyme. Proc. Natl. Acad. Sci. USA. *87*, 2516–2520.

Turner, J., Hingorani, M.M., Kelman, Z., and O'Donnell, M. (1999). The internal workings of a DNA polymerase clamp-loading machine. EMBO J. *18*, 771–783.

Vetter, I.R., and Wittinghofer, A. (1999). Nucleoside triphosphate-binding proteins: different scaffolds to achieve phosphoryl transfer. Q. Rev. Biophys. *32*, 1–56.

Walker, J.E., Saraste, M., Runswick, M.J., and Gay, N.J. (1982). Distantly related sequences in the alpha- and beta-subunits of ATP synthase, myosin, kinases and other ATP-requiring enzymes and a common nucleotide binding fold. EMBO J. *1*, 945–951.

Young, M.C., Reddy, M.K., and von Hippel, P.H. (1992). Structure and function of the bacteriophage T4 DNA polymerase holoenzyme. Biochemistry *31*, 8675–8690.

Yu, R.C., Hanson, P.I., Jahn, R., and Brunger, A.T. (1998). Structure of the ATP-dependent oligomerization domain of N-ethylmaleimide sensitive factor complexed with ATP. Nat. Struct. Biol. *5*, 803–811.

Yuzhakov, A., Turner, J., and O'Donnell, M. (1996). Replisome assembly reveals the basis for asymmetric function in leading and lagging strand replication. Cell *86*, 877–886.

Zhang, X., Shaw, A., Bates, P.A., Newman, R.H., Gowen, B., Orlova, E., Gorman, M.A., Kondo, H., Dokurno, P., and Lally, J. (2000). Structure of the AAA ATPase p97. Mol. Cell *6*, 1473–1484.

Accession Numbers

Coordinates have been deposited with the Protein Data Bank under the accession codes 1JR3.